A Two-Axis Electrothermal Micromirror for Endoscopic Optical Coherence Tomography

Ankur Jain, *Student Member, IEEE*, Anthony Kopa, *Student Member, IEEE*, Yingtian Pan, Gary K. Fedder, *Senior Member, IEEE*, and Huikai Xie, *Member, IEEE*

***Abstract*—This paper reports a 1-mm^2, two-axis, single-crystalline-silicon (SCS)-based aluminum-coated scanning micromirror with large rotation angle (up to 40°), which can be used in an endoscopic optical coherence tomography imaging system. The micromirror is fabricated using a deep reactive ion etch post-CMOS micromachining process. The static response, frequency response, resonance frequency shift, and thermal imaging of the device are presented. A 4×4 pixel display using this two-dimensional micromirror device has been demonstrated.**

***Index Terms*—Electrothermal actuation, microactuators, optical coherence tomography, optical scanners, two-dimensional (2-D) mirrors.**

I. Introduction

OPTICAL coherence tomography (OCT) is an emerging medical imaging technology that produces high-resolution cross-sectional images of biological samples [1]. OCT exploits the short temporal coherence of a near-infrared broad-band light source and can image the cellular structure of tissues at depths greater than conventional microscopes. It is noninvasive and has the potential to reduce or guide invasive and time-consuming biopsy procedures. Another very attractive feature of OCT imaging is the high resolution. An OCT system with 1-μm axial resolution has been demonstrated [2], which is about two orders of magnitude higher than that of ultrasound imaging. Infrared light is also much safer than X-rays.

OCT has been proved to be clinically useful in the field of ophthalmology, and has great potential for use in cardiovascular, gastrointestinal, and pulmonary imaging through the use of endoscopes and catheters [3]. Endoscopic OCT systems have been used to detect cancers at a very early stage [4], [5]. For these internal organ applications, the imaging probe must be small, and fast image scanning is required. Various methodologies have been proposed to transversely scan the optical beam across the internal tissue surface. Some endoscopic OCT devices use a rotating hollow cable that carries a single-mode optical fiber, while others use a galvanometric plate or piezoelectric transducer that swings the distal fiber tip to perform *in vivo* transverse scanning of tissue [5]–[7].

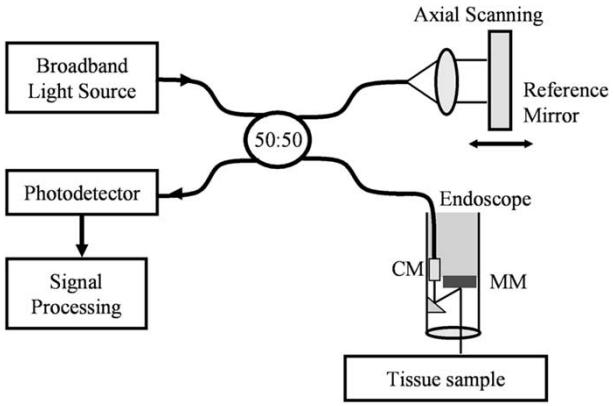

Fig. 1. Schematic of a MEMS-based endoscopic OCT system. CM: collimator. MM: micromirror.

Microsystem technology (MST) [also called microelectromechanical systems (MEMS)] is another emerging technology that makes miniature sensors and actuators. MEMS mirrors have been widely used for optical displays and optical switching. The small size, fast speed, and low power consumption of MEMS mirrors make them ideal for use in an endoscopic OCT imaging probe. In fact, researchers have started to use MEMS mirrors for the transverse scanning of endoscopic OCT systems [8], [9]. The authors have previously demonstrated a 5-mm-diameter MEMS-based OCT endoscope that used a one-dimensional (1-D) electrothermal mirror to scan the light beam onto the biological tissue [8]. By performing 1-D transverse scans of the tissue, high-resolution cross-sectional two-dimensional (2-D) images were obtained. Fig. 1 shows a schematic of a MEMS-based OCT setup. The collimated light in the sample arm of the Michelson's interferometer is reflected off the beam steering micromirror and focused into the tissue. The same mirror collects the backscattered light from the tissue, and the tissue microstructure is determined by low-coherence interferometry when scanning tissue in-depth and laterally. Zara *et al.*also reported a MEMS-based OCT probe [9].

However, the 1-D transverse scanning along with the axial scanning can only generate 2-D images. Therefore, the whole imaging probe has to be moved to scan an area of an internal organ, so the imaging efficiency is low. Some other drawbacks of these single-axis transverse-scanning probes include the complexity and inaccuracies involved in repositioning the

Manuscript received October 17, 2003; revised March 23, 2004. This work was supported in part by the NASA University of Central Florida/University of Florida Space Research Initiative and in part by the Florida Photonics Center of Excellence.

A. Jain, A. Kopa, and H. Xie are with the Department of Electrical and Computer Engineering, University of Florida, Gainesville, FL 32611 USA (e-mail: ajain@ufl.edu; hkxie@ece.ufl.edu).

Y. Pan is with the Department of Biomedical Engineering, State University of New York, Stony Brook, NY 11794 USA.

G. K. Fedder is with the Department of Electrical and Computer Engineering and the Institute of Robotics, Carnegie Mellon University, Pittsburgh, PA 15213 USA.

Digital Object Identifier 10.1109/JSTQE.2004.829194

probe at adjacent tissue locations in order to successfully map the tissue structure in three dimensions, thereby giving clinicians a better picture about the tissue microstructure.

In order to obtain the desired three-dimensional (3-D) OCT images, the beam steering mechanism must scan the tissue in the two transverse directions. Using a micromirror to scan in two dimensions will result in faster imaging speeds and more efficient scans.

Numerous designs have been proposed in the literature for performing 2-D scans using micromirrors. These 2-D micromirrors are actuated by electromagnetic, piezoelectric, or electrostatic techniques [10]–[17]. Electromagnetically actuated mirrors can achieve large rotation angles of $\pm 15.7^{\circ}$ [10], and $\pm 18^{\circ}$ [11], but they require large external magnets for actuation. Therefore, packaging this device in an endoscope or catheter is a challenge. Two-dimensional electrostatic mirrors have been reported to produce mechanical rotation angles of $\pm 5.5^{\circ}$ at a resonant frequency of 720 Hz [12], up to $\sim 10^{\circ}$ at 100 V [13], $\pm 6.2^{\circ}$ at 55 V [14], and $\pm 7.5^{\circ}$ [15]. Although the high resonant frequencies of electrostatic mirrors allow for high-speed scanning, the scan area is limited by the small rotation angles. Also, the high voltages required for larger angular actuation are a deterring factor in their use for internal *in vivo* imaging. Piezoelectrically actuated micromirrors with rotation angles of 2.3° at 4.5 V [16] and 5.5° at 16 V [17] have been reported, but they are also limited to the area they can scan. Therefore, these aforementioned mirror designs may not be ideal for an endoscopic OCT probe, as they do not meet all the probe requirements of small size, fast scanning speed, ease of packaging, and low cost of fabrication. The micromirror must also be large and flat to maintain high light coupling efficiency and spatial resolution and should also have large angles of rotation to image large areas.

In this paper, we present an electrothermally actuated single-crystal-silicon (SCS)-based 2-D micromirror, designed to address the scanning requirements of an endoscopic OCT system. The mirror is fabricated by using a deep reactive ion etch (DRIE) CMOS–MEMS process [18]. This fabrication process provides thick SCS structures for mirror flatness. An SCS mirror with a large radius of curvature of 50 cm has been reported [8]. The fabrication process also provides mechanical thin-film bimorph beams, which allow for large actuation angles. The authors have previously reported large mirror rotation angles of 17° [8] and 31° [19] at <20 V dc, by electrothermally actuating the thin-film bimorph actuators. Resonant frequencies of about 0.5 kHz have been achieved with these structures. The fabricated 2-D micromirror can rotate more than 25° along both axes. The advantages of these MEMS micromirrors include large rotation angles at low voltages, high scanning speed, small device size that allows for easy insertion into an endoscope, and potential low cost due to the simple fabrication process. In this paper, we first briefly introduce the fabrication process flow in Section II. The 2-D micromirror design is then presented in Section III, while Section IV describes its characterization. The laser scanning experiment using the 2-D mirror is presented in Section V.

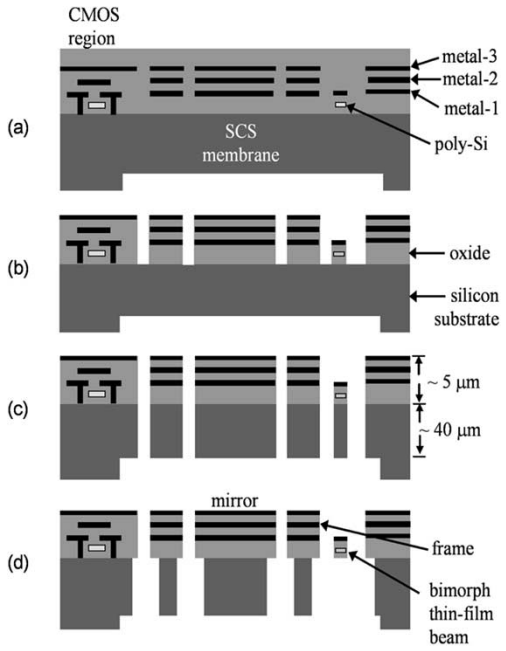

Fig. 2. DRIE CMOS–MEMS process flow. (a) Backside etch. (b) Oxide etch. (c) Deep Si etch. (d) Si undercut.

II. DRIE CMOS–MEMS Process

The device is fabricated using a four-step, post-CMOS DRIE–MEMS process [18], which is shown in Fig. 2. The process starts with a backside deep anisotropic silicon etch to form a 40-μm-thick SCS membrane. This SCS membrane is required to keep the mirror flat. The second step is a frontside anisotropic oxide etch that uses the interconnect metal (i.e., aluminum) as an etching mask. Next, a deep silicon trench etch is done to release the microstructure. The last step is an isotropic silicon etch, performed to undercut the silicon to form bimorph thin-film beams which are ~ 2 μm thick. These thin-film beams provide z-axis compliance for out-of-plane actuation, and form bimorph actuators with embedded polysilicon heater. There are no substrate or thin-film layers directly above or below the mirror microstructure, so large actuation range is allowed. As the top aluminum layer is used as an etching mask, CMOS circuits under it will remain unaffected by the fabrication process. Therefore, CMOS circuits can be integrated with the MEMS device. This process is maskless, uses only dry etch steps, and is completely compatible with foundry CMOS processes.

III. Device Description

The schematic drawing of the 1-mm^2 micromirror device is illustrated in Fig. 3. The mirror is attached to a movable frame by a set of bimorph aluminum/silicon dioxide thin-film beams. A polysilicon resistor is embedded within the silicon dioxide layer to form the bimorph thermal actuator. As this set of bimorph thin-film beams directly actuates the mirror, it is referred to as the *mirror actuator*. The movable frame is connected to the silicon substrate by another set of identical bimorph thin-film beams that are oriented perpendicular to the first. This second

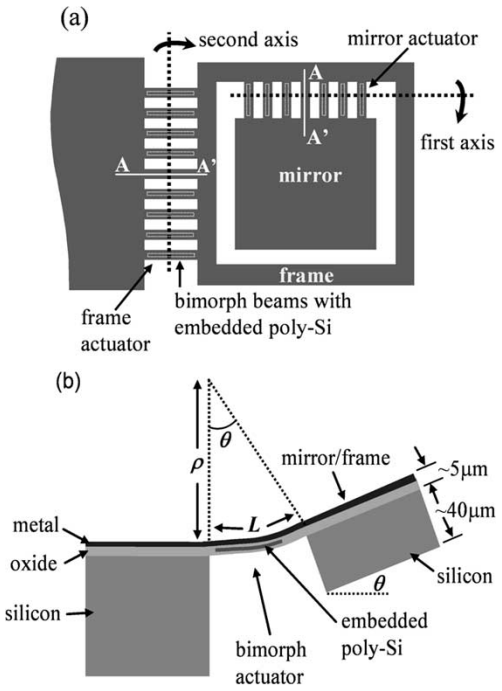

Fig. 3. Schematic of the mirror design. (a) Top view showing axes of rotation. (b) Cross-sectional view of A and A′ in Fig. 3(a). This schematic is not a true representation of the actual number of bimorph thin-film beams that comprise the thermal actuators.

set of bimorph beams actuates the frame, and is referred to as the *frame actuator*. The orthogonal orientation of the two actuators results in two perpendicular axes of rotation for the mirror.

Each side of the rectangular frame is 75 μm wide, and as seen from Fig. 2(c), the frame has a 40-μm-thick SCS layer under it to provide rigidity to the structure. After the mirror is released during fabrication, the bimorph actuators have initial curling due to the residual stresses in the aluminum and silicon dioxide layers. The initial tilt angles of the mirror and frame due to the curling of the thermal actuators can be calculated from $\theta = L/\rho$, where θ is the initial tilt angle and L and ρ are the lengths and radii of curvature of the thermal actuators, respectively.

The heating element in the bimorph beams is a set of 200-μm-long, 7-μm-wide polysilicon strips oriented along the beams. This narrow polysilicon width is selected to reduce the process time for the silicon undercut [Fig. 2(d)]. The CMOS process permits a maximum current of $\sim$1 mA per micrometer width of polysilicon. Therefore, only a maximum current of 7 mA can flow through each individual bimorph beam. In order to increase this current limit to a higher value, the polysilicon resistors in two adjacent beams are connected in parallel. This results in a beam pair resistance of 34 Ω. The fabricated mirror has 32 and 38 pairs of bimorph beams in the mirror and frame actuators, respectively. This gives us mirror and frame actuator resistances of 1.1 and 1.3 kΩ, respectively. When the applied current through the embedded polysilicon resistor is increased during actuation, the temperature in the bimorph actuator increases. Since the thermal coefficient of expansion of aluminum (23.1 μstrain/K) is greater than that of silicon dioxide (0.7 μstrain/K) [20], the bimorph beams bend downward, and this results in a downward angular displacement of the attached mirror.

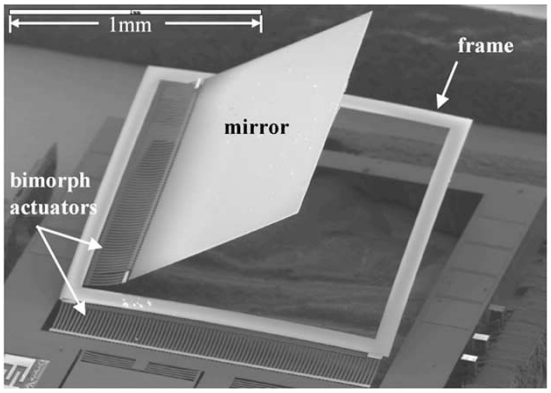

Fig. 4. SEM of a fabricated 2-D mirror.

As shown in the cross-sectional view of the device [Fig. 3(b)], the top layer of the mirror is an interconnect metal layer (i.e., aluminum). Thus, the mirror has high reflectivity. A 40-μm-thick SCS layer backing the mirror plate guarantees the mirror flatness. Large, optically flat mirrors are required to maintain high light coupling efficiency and spatial resolution. The fabricated mirror size 1 mm $\times$ 1 mm is chosen to fit the available space in the OCT imaging probe.

Fig. 4 shows a scanning electron micrograph (SEM) of a fabricated micromirror. The mirror tilts 42° and the frame tilts 16°, at room temperature, with respect to the substrate. These initial tilt angles are due to the residual stresses present in the bimorph beams. The maximum actuation angles allowed by this device design are limited by the substrate contact points. Calculations based on a 500-μm-thick wafer show that the mirror can tilt up to $-22°$, while the frame can tilt up to $-17°$ below the wafer surface. Therefore, the maximum allowed rotation angles for the mirror and frame are 64° and 33°, respectively.

IV. Characterization

Various experiments were performed to determine the characteristics of this device. These experiments include static response, frequency response, resonance frequency shift, long-term device reliability, and thermal imaging of the device.

A. Angular Rotation Versus Applied Current

An experimental setup with a laser beam incident on the mirror and dc current supplied to the two actuators was used to measure the static deflection angles. The mechanical scan angle of the mirror was obtained by measuring the displacement of this incident laser beam. Fig. 5(a) shows the measured angles of rotation at different currents for the two independent axes. The mirror rotates 40° at an applied current of 6.3 mA (or 15 V, corresponding to an applied power of 95 mW), while the frame rotates by 25° at a current of 8 mA (or 17 V, corresponding to a power of 135 mW). Mirror rotation angles up to 50° have been observed at higher currents, but the high stress induced in the bimorph actuator results in mirror instability. It has been observed that thermal damage in the polysilicon heater occurs

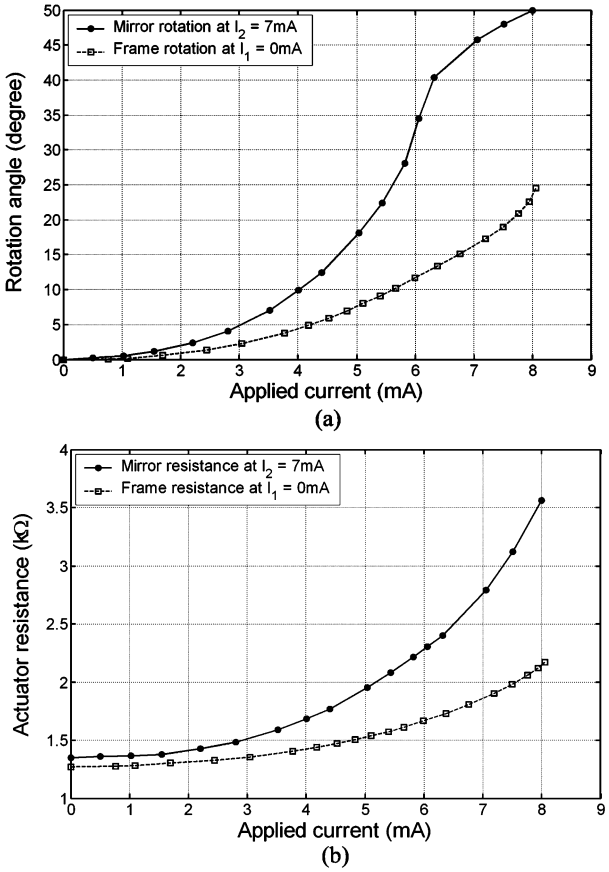

Fig. 5. (a) Rotation angle versus current for the two actuators. (b) Polysilicon resistance versus current for the two actuators. I_1: current in mirror actuator. I_2: current in frame actuator. A 7-mA frame actuator current is required for aligning the rotation axis of the mirror actuator with the substrate.

at this point. The bimorph actuators burn out at an applied voltage of 28 V; this corresponds to burnout currents of 8 and 11 mA in the mirror and frame actuators, respectively. The mirror instability limits the usable scan range of the mirror actuator to 40°.

Due to the large angular displacements by the actuators, the center of the mirror plate does not remain stationary in the vertical direction. At a rotation angle of 20° (optical angle of 40°), the center of the mirror plate displaces by 170 μm along the probe laser-beam axis, which generates additional optical path length in the sample arm of the OCT system in Fig. 1. This optical path length increase (within 200 μm) will be compensated by increasing the scan length of the axial-scanning reference mirror.

B. Actuator Resistance Versus Applied Current

The temperature increase in the bimorph actuators during actuation is proportional to their thermal resistance. The thermal resistance of the actuators depends on the heat-flow path from the actuators to the substrate. Since the mechanical structure of the frame provides additional thermal isolation to the mirror actuator, the mirror actuator has a larger thermal resistance to the silicon substrate than the frame actuator. Therefore, the same actuation current will cause larger angular rotation by the mirror actuator than by the frame actuator. The dc current dependence of the resistors is plotted in Fig. 5(b). The resistances of the polysilicon heaters change significantly with current because the heating effect of the current causes temperature change, which in turn induces stress change in the bimorph beams. The measured open circuit polysilicon resistances of the mirror and frame actuators are 1.09 and 1.26 kΩ, respectively.

C. Temperature Analysis

The temperature distribution on the surface of the device was observed using an infrared thermal camera. The temperature distribution profile of the entire mirror actuator is shown in Fig. 6(a). Fig. 6(b) shows this distribution over the entire device, and as expected, the mirror actuator has a higher temperature than the frame actuator due to the thermal isolation provided by the frame. Even though the actuator temperatures can be as high as 120 °C, the mirror plate and silicon substrate dissipate heat and remain at relatively lower temperatures ($\sim$40 °C). The mirror is packaged inside an OCT endoscope, as seen in Fig. 1. The endoscope provides a heat flow path so that there is no significant increase in the temperature of the probe during extended periods of usage, so there will be no thermal damage to tissue during imaging.

D. Frequency Response

The resonant frequencies of the mirror and frame actuator structures were measured to be 445 and 259 Hz, respectively. It has been observed that the resonant frequency of the mirror actuator increases with increasing bias voltage in either actuator. This is shown in Fig. 7. The increase in resonance frequency of the mirror is more pronounced with an increase in mirror actuator voltage than with an increase in the frame actuator voltage. A mirror actuator biased at 12 V increases the resonance frequency by 37%, but the resonance drift due to the change in frame actuator bias is contained to within 2%. Therefore, for stable resonance scanning of the mirror, it is desirable to operate this device at a higher mirror actuator bias, as this will result in least drift of the resonance peak.

E. Long-Term Reliability

The long-term reliability of the mirror was evaluated by scanning the mirror to steer a laser beam onto a fixed screen. The mirror was continuously scanned at 5 Hz, and the scan length and angular position of the reflected laser beam were measured for over 2 million cycles. For the entire duration of the experiment, the observed angular drift was about 0.8°, which is mostly due to fluctuations in ambient temperature.

The radius of curvature of the mirror was measured by a Wyko white light profilometer to be 0.33 m. The mirror can be made optically flatter by using a thicker SCS layer backing the mirror plate or by depositing stress-compensating layers under the top reflective aluminum layer.

V. Laser Scanning Experiment

To further study the scanning behavior of the 2-D micromirror, a laser scanning experiment was performed [21],

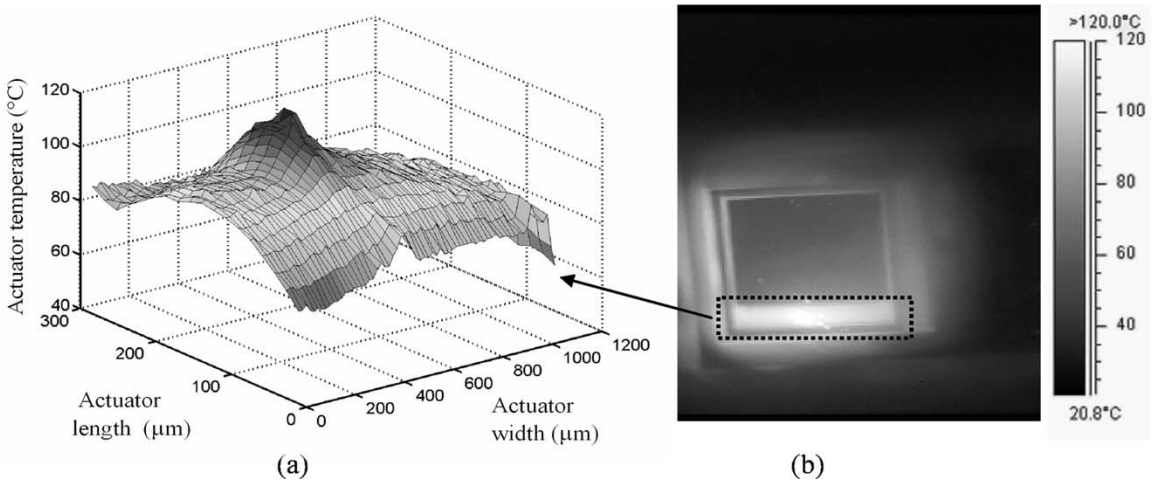

Fig. 6. Thermal images of a device biased at 10 V. (a) Temperature distribution across the mirror actuator only [highlighted in (b)]. (b) Thermograph of the entire device.

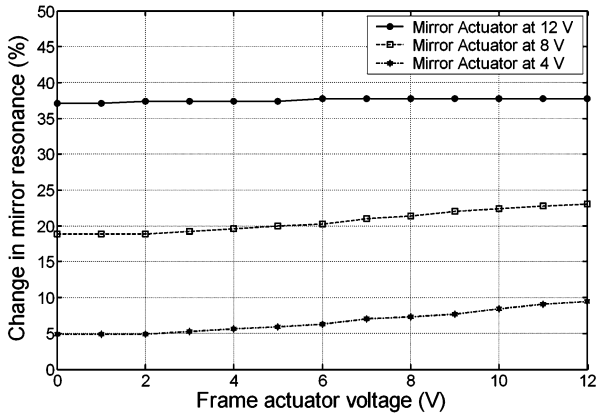

Fig. 7. Percentage increase in resonant frequency of mirror at different frame actuator voltages.

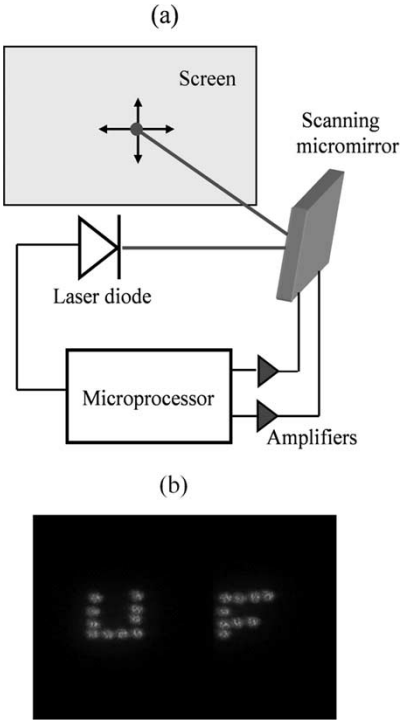

Fig. 8. (a) Setup of the laser beam scanning experiment. (b) 4×4 pixel images scanned by the micromirror.

which simulates the 2-D transverse scanning for 3-D OCT imaging. This laser scanning application, as opposed to OCT imaging, is not affected by the axial translation of the scanning mirror.

In this experiment, a simple visual display was successfully demonstrated by using this 2-D micromirror. The objective of this beam scanning experiment was to scan a pixel field with the micromirror and then to illuminate the selected pixels with a laser diode, thereby creating a projection display. The experimental setup is shown in Fig. 8(a). By using a microprocessor to control the mirror and laser, a display resolution of 4×4 pixels at 10 frames/s was demonstrated. A sample image projected on a screen is shown in Fig. 8(b). An active notch filter was incorporated into the amplifier to remove frequency content from the driving signals, which could excite the mirror's resonant vibration modes. The 4×4 pixel resolution is largely limited by attempts to stabilize the mirror for each pixel.

A new technique is currently in development to use the device in a continuous resonant scanning mode, in a scan pattern similar to that of a raster scan. This would simplify the motion of the mirror and allow for better resolution and higher frame rates.

VI. Conclusion

A large electrothermal 2-D micromirror was successfully demonstrated. The fabrication process is simple and compatible with CMOS processes; therefore, control circuits can be integrated with the mirror on the same chip. The low driving voltage and large rotation angles make this device very suitable for laser scanning endoscopic imaging systems and for optical display applications. The techniques and models that are being developed for a high-resolution projection display will be directly employed to control the laser beam scanning in an endoscopic OCT system because the same basic operation of the device is required for both systems. Three-dimensional

endoscopic OCT imaging is being conducted and will be presented soon.

ACKNOWLEDGMENT

The authors would like to thank Dr. M. Bass and T. Chung, from CREOL, University of Central Florida, Orlando, for their assistance with the thermal imager.

REFERENCES

[1] D. Huang, E. A. Swanson, C. P. Lin, J. S. Schuman, W. G. Stinson, W. Chang, M. R. Hee, T. Flotte, K. Gregory, C. A. Puliafito, and J. G. Fujimoto, "Optical coherence tomography," *Science*, vol. 254, pp. 1178–1181, 1991.

[2] W. Drexler, U. Morgner, F. X. Kartner, C. Pitris, S. A. Boppart, X. D. Li, E. P. Ippen, and J. G. Fujimoto, "*In vivo* ultrahigh-resolution optical coherence tomography," *Opt. Lett.*, vol. 24, pp. 1221–1223, 1999.

[3] B. E. Bouma and G. J. Tearney, "Clinical imaging with optical coherence tomography," *Academ. Radiol.*, vol. 9, no. 8, pp. 942–953, 2002.

[4] T. -Q. Xie, M. L. Zeidel, and Y. -T. Pan, "Detection of tumorigenesis in urinary bladder with optical coherence tomography: Optical characterization of morphological changes," *Opt. Express*, vol. 10, no. 24, pp. 1431–1443, 2002.

[5] A. M. Sergeev, V. M. Gelikonov, G. V. Gelikonov, F. I. Feldchtein, R. V. Kuranov, N. D. Gladkova, N. M. Shakhova, L. B. Snopova, A. V. Shakhov, I. A. Kuznetzova, A. N. Denisenko, V. V. Pochinko, Y. P. Chumakov, and O. S. Streltzova, "In vivo endoscopic OCT imaging of precancer and cancer states of human mucosa," *Opt. Express*, vol. 1, pp. 432–440, 1997.

[6] G. J. Tearney, M. E. Brezinski, B. E. Bouma, S. A. Boppart, C. Pitris, J. F. Southern, and J. G. Fujimoto, "In vivo endoscopic optical biopsy with optical coherence tomography," *Science*, vol. 276, pp. 2037–2039, 1997.

[7] S. A. Boppart, B. E. Bouma, C. Pitris, G. J. Tearney, J. G. Fujimoto, and M. E. Brezinski, "Forward-imaging instruments for optical coherence tomography," *Opt. Lett.*, vol. 22, pp. 1618–1620, 1997.

[8] H. Xie, Y. Pan, and G. K. Fedder, "Endoscopic optical coherence tomographic imaging with a CMOS–MEMS micromirror," *Sens. Actuators A, Phys.*, vol. 103, pp. 237–241, 2003.

[9] J. M. Zara, J. A. Izatt, K. D. Rao, S. Yazdanfar, and S. W. Smith, "Scanning mirror for optical coherence tomography using an electrostatic MEMS actuator," in *Proc. IEEE Int. Symp. Biomedical Imaging*, 2002, pp. 297–300.

[10] I. -J. Cho, K. -S. Yun, H. -K. Lee, J. -B. Yoon, and E. Yoon, "A low-voltage two-axis electromagnetically actuated micromirror with bulk silicon mirror plates and torsion bars," in *Proc. 15th IEEE Int. Conf. MEMS*, 2002, pp. 540–543.

[11] J. Bernstein, W. P. Taylor, J. Brazzle, G. Kirkos, J. Odhner, A. Pareek, and M. Zai, "Two axis-of-rotation mirror array using electromagnetic MEMS," in *Proc. 16th Annu. Int. Conf. MEMS*, 2003, pp. 275–278.

[12] H. Schenk, P. Durr, D. Kunze, H. Lakner, and H. Kuck, "An electrostatically excited 2D-micro-scanning-mirror with an in-plane configuration of the driving electrodes," in *Proc. 13th Annu. Int. Conf. MEMS*, 2000, pp. 473–478.

[13] S. Kwon, V. Milanovic, and L. P. Lee, "A high aspect ratio 2D gimbaled microscanner with large static rotation," in *Proc. 2002 IEEE/LEOS Int. Conf. Optical MEMS*, pp. 149–150.

[14] W. Piyawattanametha, P. R. Patterson, D. Hah, H. Toshiyoshi, and M. C. Wu, "A 2D scanner by surface and bulk micromachined angular vertical comb actuators," in *2003 IEEE/LEOS Int. Conf. Optical MEMS*, pp. 93–94.

[15] G.-D. Su, H. Toshiyoshi, and M. C. Wu, "Surface-micromachined 2-D optical scanners with high-performance single-crystalline silicon micromirrors," *IEEE Photon. Technol. Lett.*, vol. 13, pp. 606–608, June 2001.

[16] T. Kawabata, M. Ikeda, H. Goto, M. Matsumoto, and T. Yada, "The 2-dimensional micro scanner integrated with PZT thin film actuator," in *Proc. Transducers '97*, pp. 339–342.

[17] S. J. Kim, Y. H. Cho, H. J. Nam, and J. U. Bu, "Piezoelectrically pushed rotational micromirrors for wide-angle optical switch applications," in *Proc. 16th Annu. Int. Conf. MEMS*, 2003, pp. 263–266.

[18] H. Xie, L. Erdmann, X. Zhu, K. Gabriel, and G. K. Fedder, "Post-CMOS processing for high-aspect-ratio integrated silicon microstructures," *J. Microelectromech. Syst.*, vol. 11, pp. 93–101, Apr. 2002.

[19] H. Xie, A. Jain, T. Xie, Y. Pan, and G. K. Fedder, "A single-crystal silicon-based micromirror with large scanning angle for biomedical applications," presented at the 23rd Annu. Conf. Lasers and Electro-Optics (CLEO 2003), Baltimore, MD.

[20] D. Senturia, *Microsystem Design*. Boston, MA: Kluwer, 2001, pp. 196–196.

[21] A. Kopa, A. Jain, and H. Xie, "Laser scanning display using a 2D micromirror," presented at the Optics in the Southeast 2003, Orlando, FL.

Ankur Jain (S'03) was born in Calcutta, India, in 1977. He received the B.E. (honors) degree in electrical and electronics from the Birla Institute of Technology and Science (BITS), Pilani, India, in 2000. He received the M.S. degree in electrical engineering from the University of Florida, Gainesville, in 2002, and is currently working toward the Ph.D. degree in the Department of Electrical and Computer Engineering,University of Florida.

His research interests include microelectromechanical systems (MEMS), endoscopic optical coherence tomography, biomedical imaging, and photonic devices.

Mr. Jain is a Student Member of the Optical Society of America. He is a Member of Eta Kappa Nu and Tau Beta Pi. He was awarded the Motorola Student of the Year gold medal for 2000.

Anthony Kopa (S'03) received the A.A. degree (with highest honors) from Indian River Community College, Fort Pierce, FL, in 2001. He is currently working toward the B.S. and M.S. degrees in electrical engineering at the University of Florida, Gainesville.

In 2002, he was an Engineering Intern at Harbor Branch Oceanographic Institute, Fort Pierce. His research interests include optical MEMS, integrated optics, and optoelectronics.

Mr. Kopa is a Student Member of the International Society for Optical Engineering. He is a Member of Phi Theta Kappa and is a National Merit Scholar.

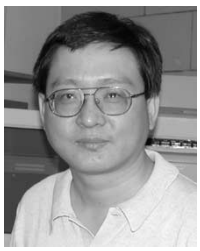

Yingtian Pan is an Assistant Professor in the Department of Biomedical Engineering, State University of New York, Stony Brook. He has over 40 journal publications. Since 1992, he has been working on noninvasive optical imaging and spectroscopy of biological tissue. His current research interest is in development of laser-scanning endoscopy for early cancer detection.

Gary K. Fedder (S'93–M'95–SM'01) received the B.S. and M.S. degrees in electrical engineering from the Massachusetts Institute of Technology (MIT), Cambridge, in 1982 and 1984, respectively, and the Ph.D. degree from the University of California, Berkeley, in 1994, where his research resulted in the first demonstration of multimode control of a underdamped surface-micromachined inertial device.

From 1984 to 1989, he worked at the Hewlett-Packard Company on circuit design and printed-circuit modeling. He is currently a Professor at Carnegie Mellon University, Pittsburgh, PA, holding a joint appointment with the Department of Electrical and Computer Engineering and the Robotics Institute. He serves on the Editorial Board of the *Journal of Micromechanics and Microengineering* (Institute of Physics) and as coeditor of the *Sensors Update and Advanced Micro- and Nanosystems* (Wiley–VCH) book series. He has contributed to over 100 research publications and several patents in the MEMS area. His research interests include microsensor and microactuator design and modeling, integrated MEMS manufactured in CMOS processes, and structured design methodologies for MEMS.

Dr. Fedder received the 1993 AIME Electronic Materials Society Ross Tucker Award, the 1996 Carnegie Institute of Technology G. T. Ladd Award, and the 1996 NSF CAREER Award. Currently, he is a Subject Editor for the *Journal of Microelectromechanical Systems* (IEEE/ASME).

Huikai Xie (S'00–M'02) received the B.S. and M.S. degrees in electronic engineering from Beijing Institute of Technology, Beijing, China, in 1989 and 1992, respectively, the M.S. degree in electrooptics from Tufts University, Medford, MA, in 1998, and the Ph.D. degree in electrical and computer engineering from Carnegie Mellon University, Pittsburgh, PA, in 2002.

From 1992 to 1996, he was a Research Faculty Member in the Institute of Microelectronics, Tsinghua University, Beijing, working on various silicon-based chemical and mechanical sensors. In 2001, he was with the North America Research Center, Robert Bosch Corporation, designing a six-degrees-of-freedom inertial measurement unit. He is currently an Assistant Professor in the Department of Electrical and Computer Engineering, University of Florida, Gainesville. He has contributed to over 30 technical papers. His current research interests include integrated microsensors, optical microelectromechanical systems, optical switching, biomedical imaging and sensing, and fiberoptic sensors.